

Orbital-Engineered Anomalous Hall Conductivity in Stable Full Heusler Compounds: A Pathway to Optimized Spintronics

Quynh Anh T. Nguyen,¹ Thi H. Ho,^{2,3} Seong-Gon Kim,⁴ Ashwani Kumar,⁵ and Viet Q. Bui^{1*}

¹*Advanced Institute of Science and Technology, The University of Danang, 41 Le Duan, Danang, Vietnam*

²*Laboratory for Computational Physics, Institute for Computational Science and Artificial Intelligence, Van Lang University, Ho Chi Minh City, Vietnam*

³*Faculty of Mechanical - Electrical and Computer Engineering, School of Technology, Van Lang University, Ho Chi Minh City, Vietnam.*

⁴*Department of Physics & Astronomy and Center for Computational Sciences, Mississippi State University, Mississippi State, Mississippi 39762, United States*

⁵*Max-Planck-Institut für Kohlenforschung, 45470 Mülheim an der Ruhr, Germany*

*Corresponding authors: Viet Q.Bui; Email: bqviet@ac.udn.vn; mrbuiquoctviet@gmail.com

Table S1. The Anomalous Hall Conductivity ($|\sigma_{xy}|$) alongside the stability and magnetic characteristics for Co_2MnZ family. The table lists the stable phase, formation energy (ΔF in eV/atom), $|\sigma_{xy}|$ (S/Cm), total magnetic moment (M_{tot} in μ_B), spin polarization (P in %).

| Co_2MnZ | Stable phase | ΔF eV/atom | $ \sigma_{xy} $ S/Cm | M_{tot} μ_B | P % |
|--------------------------|---------------|-----------------------|--|---------------------------------------|------------------------------------|
| Co_2MnAl | $\text{l}2_1$ | -0.385 | 1647 | 4.14 | 63 |
| | | -0.356 ^a | 1631 ^b , 1600-2000 ^c | 4.04 ^b 4.01 ^f | 68 ^e |
| Co_2MnGa | $\text{l}2_1$ | -0.268 | 1046 | 4.09 | 73 |
| | | -2.237 ^a | 845-1260 ^d | 4.11 ^b , 4.05 ^f | 66 ^e , 55 ^g |
| Co_2MnB | $\text{l}2_1$ | 0.017 | 447 | 4.03 | 82 |
| | | 0.032 ^a | 598 ^b , 433 ^e | | |
| Co_2MnIn | $\text{l}2_1$ | 0.024 | 378 | 4.43 | 27 |
| | | 0.064 ^a | | 4.52 ^b | 31 ^e |
| Co_2MnGe | $\text{l}2_1$ | -0.272 | 235 | 4.99 | 99 |
| | | -0.257 ^a | 253 ^b , 228 ^e | 5.00 ^b , 5.11 ^f | 100 ^e , 90 ^g |
| Co_2MnBi | $\text{l}2_1$ | 0.222 | 218 | 5.92 | 93 |
| | | 0.227 ^a | | 5.07 ^f | |
| Co_2MnSn | $\text{l}2_1$ | -0.132 | 183 | 5.00 | 77 |
| | | -0.139 ^a | 176 ^b , 174 ^e | 5.04 ^b , 5.08 ^f | 75 ^e |
| Co_2MnAs | $\text{l}2_1$ | -0.115 | 173 | 5.62 | 33 |
| | | -0.129 ^a | 178 ^b | 5.98 ^b 4.90 ^g | |
| Co_2MnSi | $\text{l}2_1$ | -0.467 | 172 | 5.03 | 1 |
| | | -0.449 ^a | 187 ^b , 193 ^e | 5.00 ^b | 100 ^e , 93 ^g |
| Co_2MnPb | $\text{l}2_1$ | 0.217 | 31 | 5.06 | 65 |
| | | 0.240 ^a | | | |
| Co_2MnSb | $\text{l}2_1$ | -0.104 | 25 | 5.95 | 100 |
| | | -0.094 ^a | | 5.96 ^b 4.9 ^f | |

^a Theoretical data¹

^b Theoretical data²

^c Experiment data³

^d Experiment data⁴

^e Theoretical data⁵

^f Experiment data⁶

^g Experiment data⁷

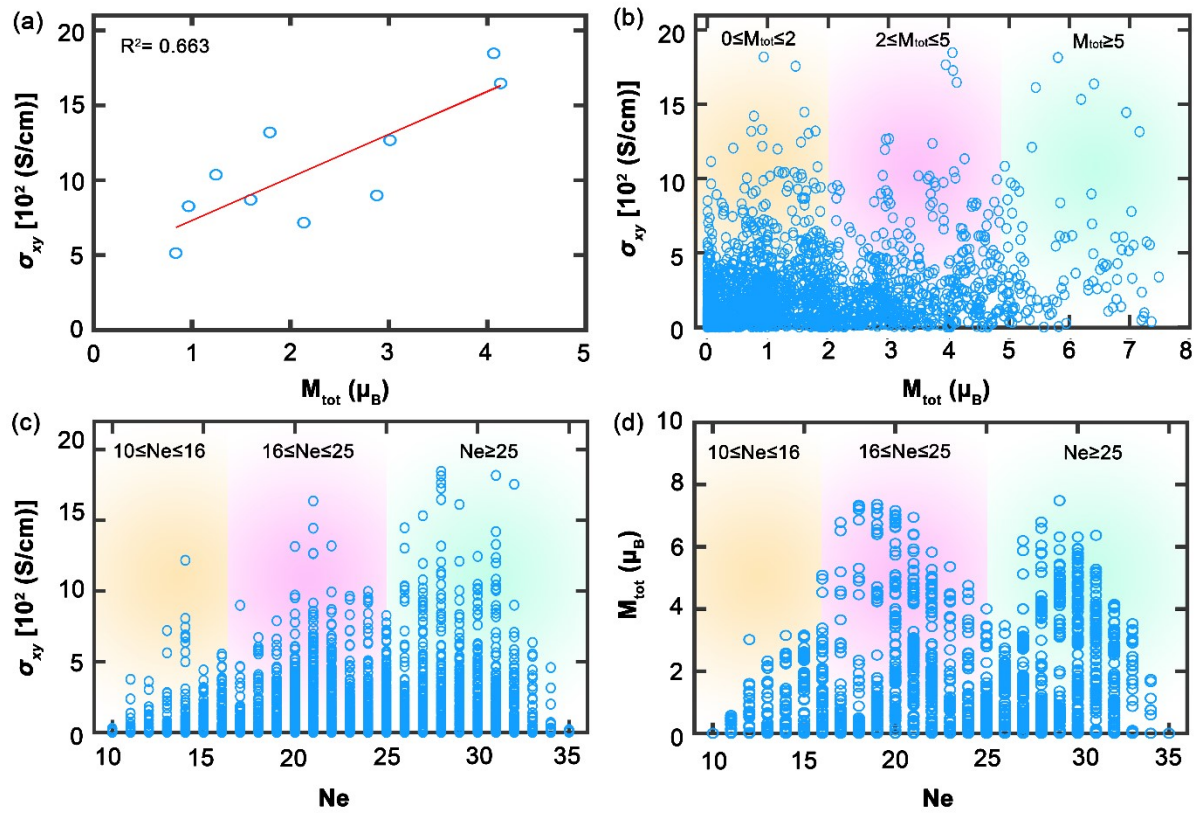


Figure S1. Anomalous Hall conductivity σ_{xy} as a function of total magnetic moment M_{tot} for data in (a) table 1 and (b) whole data. Yellow, purple, and cyan backgrounds distinguish three areas $0 \leq M_{tot} \leq 2$, $2 \leq M_{tot} \leq 5$, and $M_{tot} \geq 5$, respectively. (c) σ_{xy} and (d) M_{tot} as a function of total valance electrons Ne . Yellow, purple, and cyan backgrounds distinguish three areas $10 \leq Ne \leq 16$, $16 \leq Ne \leq 25$, and $Ne \geq 25$, respectively.

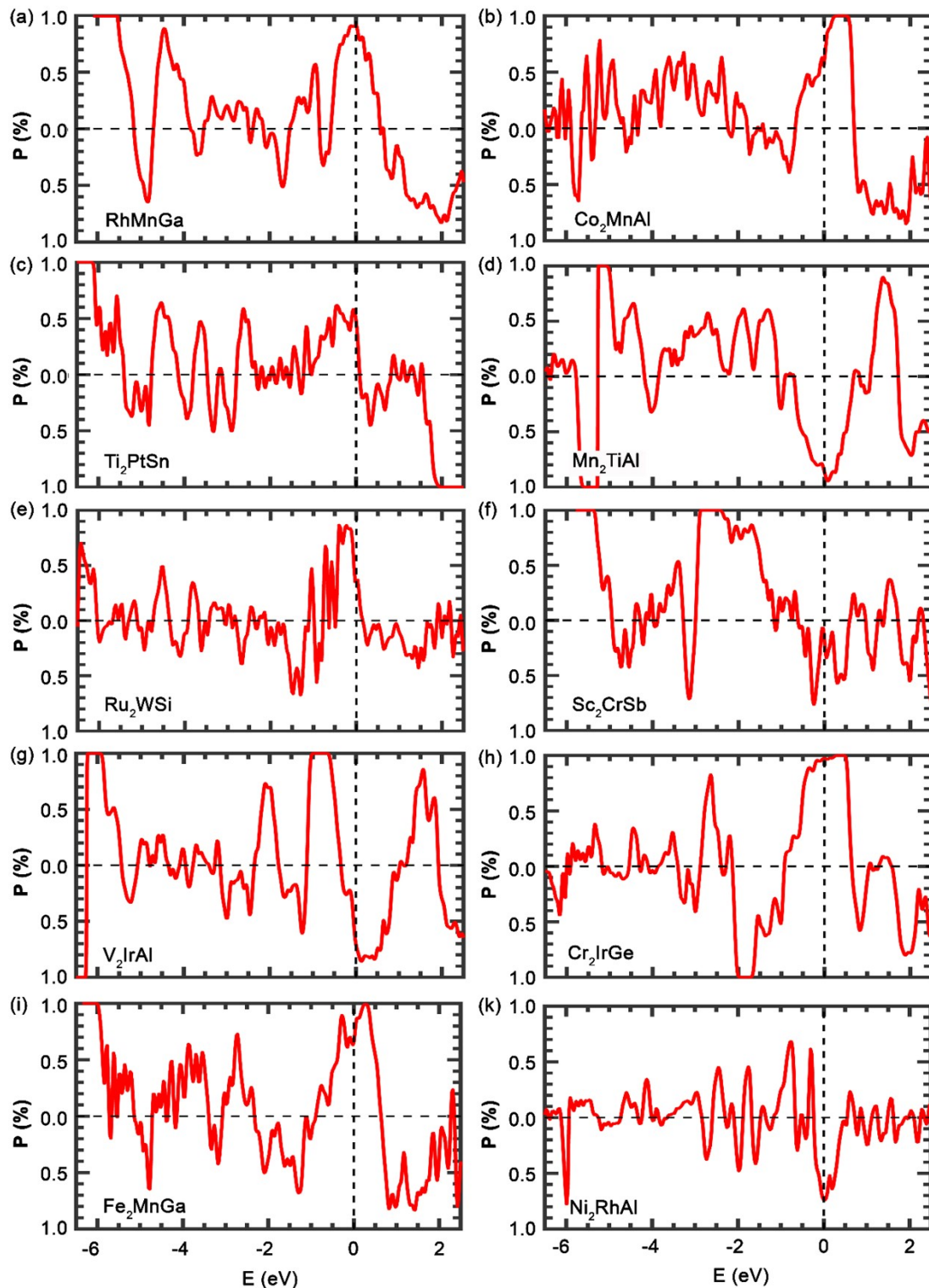


Figure S2. Spin polarization P (%) as the function of energy. for selected compounds (a) Rh₂MnGa, (b) Co₂MnAl, (c) Ti₂PtSn, (d) Mn₂TiAl, (e) Ru₂WSi, (f) Sc₂CrSb, (g) V₂IrAl, (h) Cr₂IrGe, (i) Fe₂MnGa, and (k) Ni₂RhAl. E_F is set to zero.

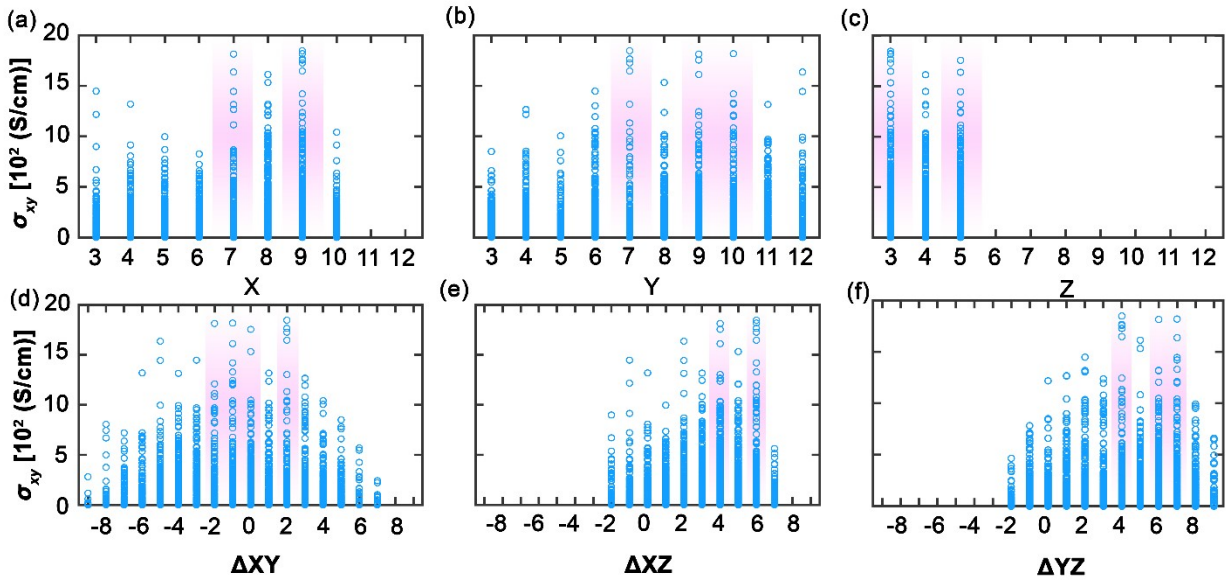


Figure S3. Anomalous Hall conductivity (σ_{xy}) as a function of valence electrons for (a) X, (b) Y, and (c) Z elements. σ_{xy} as a function of valence electron differences between (d) X and Y (ΔXY), (e) X and Z (ΔXZ), and (f) Y and Z (ΔYZ). Purple backgrounds distinguish areas exhibiting large σ_{xy} .

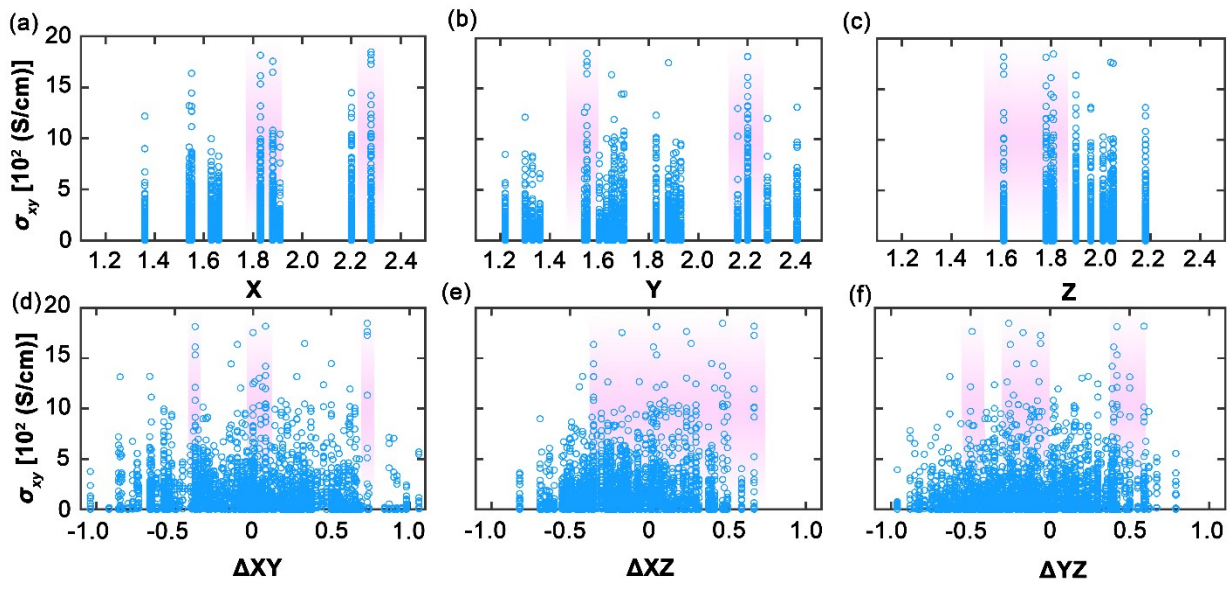


Figure S4. Anomalous Hall conductivity (σ_{xy}) as a function of electronegativity for (a) X, (b) Y, and (c) Z elements. σ_{xy} as a function of electronegativity differences between (d) X and Y (ΔXY), (e) X and Z (ΔXZ), and (f) Y and Z (ΔYZ). Purple backgrounds distinguish areas exhibiting large σ_{xy} .

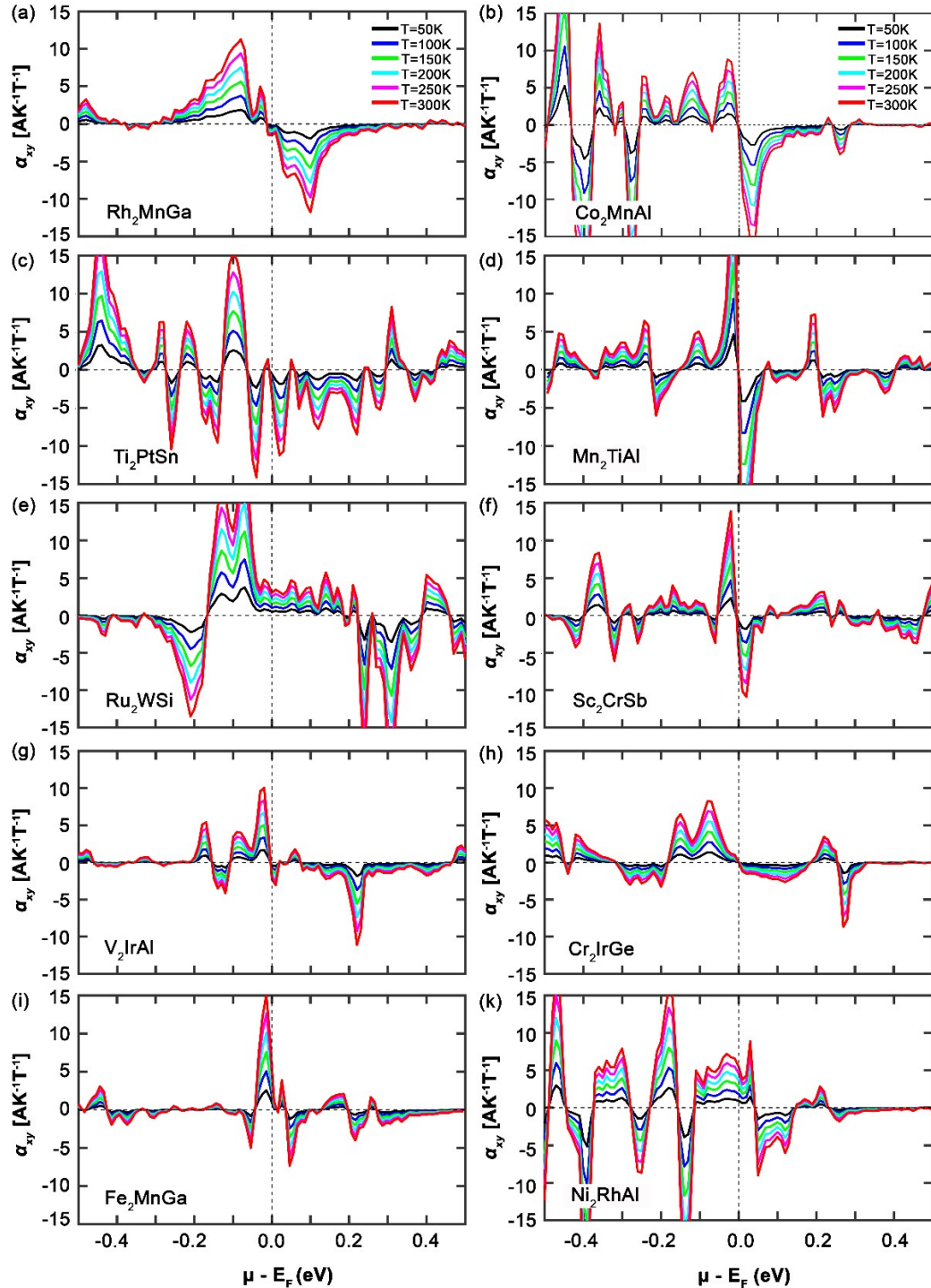


Figure S5. Anomalous Nernst conductivity (α_{xy}) as a function of chemical potential μ for selected compounds (a) Rh_2MnGa , (b) Co_2MnAl , (c) Ti_2PtSn , (d) Mn_2TiAl , (e) Ru_2WSi , (f) Sc_2CrSb , (g) V_2IrAl , (h) Cr_2IrGe , (i) Fe_2MnGa , and (k) Ni_2RhAl . E_F is set to zero.

References

1. S. Kirklin, J. E. Saal, B. Meredig, A. Thompson, J. W. Doak, M. Aykol, S. Rühl, and C. Wolverton, npj Npj Comput. Mater., 2015, **1**, 1.
2. J. Noky, Y. Zhang, J. Gooth, C. Felser, and Y. Sun, npj Npj Comput. Mater., 2020 **6**, 77.
3. E. Vilanova Vidal, G. Stryganyuk, H. Schneider, C. Felser, and G. Jakob, Appl. Phys. Lett., 2011, **99**.
4. S. N. Guin *et al.*, NPG Asia Mater., 2019, **11**, 16.
5. J.-C. Tung and G.-Y. Guo, New J. Phys., 2013, **15**, 033014.
6. P. Webster, J. Phys. Chem. Solids, 1971, **32**, 1221.
7. C. Guillemard, S. Petit-Watelot, J.-C. Rojas-Sánchez, J. Hohlfeld, J. Ghanbaja, A. Bataille, P. Le Fèvre, F. Bertran, and S. Andrieu, Appl. Phys. Lett. 2019, **115**, 12401.